

Comparison of Methods for Rational Approximation of Simulated Time-Domain Responses: ARMA, ZD-VF, and TD-VF

Andrea Ubolli, *Member, IEEE*, and Bjørn Gustavsen, *Senior Member, IEEE*

Abstract—This paper compares alternative methods for linear modeling of simulated time-domain responses by a rational approximation. The traditional approach based on autoregressive moving average (ARMA) is compared with two alternative approaches that have been introduced in recent years: Z-Domain Vector Fitting (ZD-VF) and Time-Domain Vector Fitting (TD-VF). Following a description of their implementation and fundamental properties, the methods are applied to the modeling of a frequency-dependent network equivalent. It is shown that TD-VF offers superior results in terms of accuracy and robustness, and the model has guaranteed stable poles. The ARMA approach requires higher orders than the others and the resulting model can be unstable. The ZD-VF approach is robust and gives a model with stable poles, but it produces incorrect simulation results when applied to truncated time-domain responses. The inaccuracy is caused mainly by the conversion of time-domain data into the z -domain. The fitting process of ARMA is faster than with the other approaches since it does not involve iterative pole relocations.

Index Terms—Autoregressive moving average (ARMA), frequency-dependent network equivalent (FDNE), macromodel, rational approximation, time-domain vector fitting, z -domain vector fitting.

I. INTRODUCTION

THE SIMULATION of electromagnetic transients in power systems [1] requires modeling all relevant components with sufficient accuracy, including their frequency-dependent effects. In the case of linear components, this can be easily achieved via approximation with rational functions. This approach is currently applied for the modeling of transmission lines and cables [2]–[4], high-frequency transformer terminal modeling [5], [6], and terminal equivalencing of components and subnetworks, so-called frequency-dependent network equivalents (FDNEs) [7], [8].

Traditionally, the approximation (“fitting”) with rational functions has been carried out in the frequency domain, for instance using vector fitting (VF) [9]. This domain is a natural choice since the components can in many instances be

characterized only in the frequency domain. For instance, the series impedance parameters of a transmission line can only be computed in the frequency domain, and terminal characterization of components by measurement is usually most accurately performed by frequency sweep measurements.

It is, however, also possible to characterize components and subsystems in other domains. One alternative is to transform the s -domain data into the z -domain, thereby allowing to identify an autoregressive moving average (ARMA) model via the model’s discrete differential equation. That approach has been applied for the purpose of traveling wave-based transmission line modeling [4].

The ARMA modeling approach is also directly applicable to modeling from simulated time-domain responses, which is the topic of this paper. This approach has been applied to FDNE modeling in [10], [11]. In [11], the approach was further refined by utilizing the delay effects of transmission lines for achieving a reduced-order FDNE model via the resulting sparsity in the ARMA model. Reference [12] gives a discussion of accuracy aspects regarding z -domain implementations in EMTP-type programs.

In recent years, two alternative approaches have been introduced in the field of high-speed electronics modeling: vector fitting in the z -domain (ZD-VF) [13] and in the time domain (TD-VF) [14]. ZD-VF is essentially an application of VF in the z -domain rather than the s -domain. Its application requires to convert the time-domain responses into the z -domain. TD-VF is a formulation of VF in the time domain via convolution.

In this paper we apply these new methods for use with power systems modeling. We compare ARMA, ZD-VF and TD-VF when applied to rational approximation of time-domain responses obtained via an Electromagnetic Transients Program (EMTP)-type circuit simulator [1]. The objective is to obtain a rational model in the continuous s -domain so that it can later be applied in simulations with alternative time step lengths. We first give a thorough description of the approaches and how to apply them in the context of time-domain fitting. They are next applied to the modeling of a sub-network using a high-order model. The applicability of the approaches is compared regarding accuracy, robustness, and efficiency. The effect of using truncated time responses is also investigated. In this work we deal with single-port systems but we also include one preliminary result for multiport systems (Section VIII).

II. RATIONAL MODEL

We consider the time-domain impulse response $h(t)$ of a linear time invariant (LTI) system. Let $u(t)$ and $y(t)$ denote

Manuscript received March 16, 2010; revised July 02, 2010; accepted August 27, 2010. Date of publication November 09, 2010; date of current version December 27, 2010. The work was supported in part by the Norwegian Research Council (PETROMAKS Programme) and in part by Compagnie Deutsch, FMC Technologies, Framo, Norsk Hydro, Siemens, Statoil, Total, and Vetco Gray. Paper no. TPWRD-00190-2010.

The authors are with SINTEF Energy Research, Trondheim N-7465, Norway (e-mail: andrea.ubolli@elkraft.ntnu.no; bjorn.gustavsen@sintef.no).

Color versions of one or more of the figures in this paper are available online at <http://ieeexplore.ieee.org>.

Digital Object Identifier 10.1109/TPWRD.2010.2080361

the excitation and output response, respectively. Their relation is in the time domain defined by convolution (1) and in the frequency domain ($s = a + j\omega$) by multiplication (2).

$$y(t) = \int_{-\infty}^{+\infty} h(t - \tau)u(\tau) d\tau \quad (1)$$

$$Y(s) = H(s)U(s) \quad (2)$$

It is assumed that $H(s)$ has the rational form (3a), where $\{p_{n-s}\}$, $\{r_{n-s}\}$ and r_{0-s} are the poles, residues, and constant term to be identified. The time-domain counterpart is given by (3b). N is the model order and $\delta(t)$ is the Dirac's delta function

$$H(s) = \sum_{n=1}^N \frac{r_{n-s}}{s - p_{n-s}} + r_{0-s} \quad (3a)$$

$$h(t) = \sum_{n=1}^N r_{n-s} e^{p_{n-s}t} + \delta(t)r_{0-s}. \quad (3b)$$

III. PRELIMINARIES ON z -TRANSFORM

A. Definition

Given a discrete sequence $f[k]$ of time-domain samples, the expression of the unilateral, or one-sided z -transform is given by [15], [16]

$$F(z) = \sum_{k=0}^{\infty} f[k]z^{-k}. \quad (4)$$

The definition of the z -variable is related to the s -variable by (5), where Δt is the sampling time. This transformation maps the entire left-hand s -plane inside the unit circle in the z -domain [17]

$$z = e^{s\Delta t}. \quad (5)$$

B. Bilinear Transformation

In practice, the exact mapping (5) is often replaced with the bilinear transformation (6), also known as the Tustin approximation. This transformation preserves the magnitude of the exact mapping but leads to incorrect phase information. A point lying on the unit circle in the z -domain corresponding to the frequency ω becomes ω^* (7) when mapped back on the imaginary axis in the s -domain [12]

$$z = e^{s\Delta t} = \frac{e^{s\Delta t/2}}{e^{-s\Delta t/2}} \approx \frac{1 + s\frac{\Delta t}{2}}{1 - s\frac{\Delta t}{2}} \quad (6)$$

$$\omega^* = \omega \tan\left(\omega \frac{\Delta t}{2}\right) \frac{2}{\omega \Delta t}. \quad (7)$$

C. Chirp z -Transform Algorithm (CZT)

The actual computation of the z -transform from time-domain samples can be done in an efficient way using the Chirp z -transform (CZT) algorithm [18]. Given a discrete sequence $f[k]$, $k = 0 \dots K - 1$, this algorithm evaluates the z -transform of the sequence under investigation on a spiral in the z -domain complex plane, (8), with A and W given by

$$z_i = AW^{-i} \quad i = 0 \dots M - 1 \quad (8)$$

TABLE I
MAPPING TERMS FROM z -DOMAIN TO s -DOMAIN

z -domain	s -domain
r_{n-z}	$r_{n-s} = \frac{4}{\Delta t} r_{n-z} \frac{1}{(p_{n-z} + 1)^2}$
p_{n-z}	$p_{n-s} = \frac{2(p_{n-z} - 1)}{\Delta t(p_{n-z} + 1)}$
r_{0-z}	$r_{0-s} = r_{0-z} - \sum_{n=1}^N \frac{r_{n-z}}{p_{n-z} + 1}$

$$A = A_0 e^{j2\pi\beta_0} \quad W = W_0 e^{j2\pi\varphi_0}. \quad (9)$$

In our case, the spiral is part of the circumference of a unitary ray in the z -domain. Accordingly, A_0 and W_0 become unity.

Introducing z_i (8) in (4), we obtain, after manipulating the summation and defining new other two variables ν and η (10), the final result

$$\nu[n] = W^{-n^2/2}, \quad \eta[n] = f[n]A^{-n}W^{\frac{n^2}{2}}, \quad n = 0 \dots K - 1 \quad (10)$$

$$F(z_i) = W^{\frac{i^2}{2}} \left[\sum_{k=0}^{K-1} \eta(k)\nu(i-k) \right], \quad i = 0 \dots M - 1. \quad (11)$$

Thus, the computation of the z -transform can be formulated as a discrete convolution product which can be efficiently computed using fast Fourier transform (FFT).

D. Relation Between Rational Functions in z -Domain and s -Domain

A rational function can be expressed in the z -domain. In the case of simple pole-residue fractions, we obtain

$$H(z) = r_{0-z} + \sum_{n=1}^N \frac{r_{n-z}}{z - p_{n-z}}. \quad (12)$$

Using the bilinear transformation (6), the model (12) can be directly converted into the s -domain (3a) (and vice-versa). Inserting the bilinear transformation into (12) we get for the transfer function in the s -domain

$$H(s) \approx r_{0-z} - \sum_{n=1}^N \frac{r_{n-z}}{1 + p_{n-z}} + \sum_{n=1}^N \frac{\frac{4}{\Delta t} r_{n-z} \frac{1}{(1+p_{n-z})^2}}{s - \frac{2(p_{n-z}-1)}{\Delta t(p_{n-z}+1)}}. \quad (13)$$

From (13), the mapping of model parameters becomes as shown in Table I. (The mapping from the s -domain to z -domain is shown in Table II). The bilinear transformation also implies trapezoidal integration of the first-order differential equation corresponding to the state-space model (3a) [19].

IV. ARMA MODEL

A. Formulation in Time Domain and z -Domain

The convolution (1) can be represented by a linear difference equation with constant coefficients. With a fixed time step, we

TABLE II
MAPPING TERMS FROM s -DOMAIN TO z -DOMAIN

s -domain	z -domain
r_{n_s}	$r_{n_z} = r_{n_s} \Delta t \left(1 - \frac{\Delta t}{2} p_{n_s}\right)^{-2}$
p_{n_s}	$p_{n_z} = \left(1 + \frac{\Delta t}{2} p_{n_s}\right) \left(1 - \frac{\Delta t}{2} p_{n_s}\right)^{-1}$
r_{0_s}	$r_{0_z} = r_{0_s} + \sum_{n=1}^N r_{n_s} \left(\frac{2}{\Delta t} - p_{n_s}\right)^{-1}$

get for an N th-order model the relation [15]–[17]

$$\begin{aligned}
 y(t_k) = & b_0 u(t_k) + b_1 u(t_{k-1}) \\
 & + b_2 u(t_{k-2}) + \dots + b_N u(t_{k-N}) + \\
 & - a_1 y(t_{k-1}) - a_2 y(t_{k-2}) + \dots - a_N y(t_{k-N})
 \end{aligned} \quad (14)$$

where t_k is the time at the k th step while $\{a_i\}$ and $\{b_i\}$ are constant coefficients. Equation (14) describes a *long convolution* where the current output response $y(t_k)$ depends on the current excitation $u(t_k)$ as well as the N past excitations and output responses.

By applying the z -transform to (14) and using the delay operator (5), we obtain

$$\begin{aligned}
 Y(z) = & b_0 U(z) + b_1 U(z)z^{-1} \\
 & + b_2 U(z)z^{-2} + \dots + b_N U(z)z^{-N} + \\
 & - a_1 Y(z)z^{-1} - a_2 Y(z)z^{-2} + \dots - a_N Y(z)z^{-N}.
 \end{aligned} \quad (15)$$

From (15), we obtain the resulting z -domain rational transfer function (16), also known as the ARMA model. The actual computation of the model's parameters is done by solving (14) as a linear overdetermined system, more about this is in Section IV-B

$$H(z) = \frac{Y(z)}{U(z)} = \frac{b_0 + b_1 z^{-1} + b_2 z^{-2} + \dots + b_N z^{-N}}{1 + a_1 z^{-1} + a_2 z^{-2} + \dots + a_N z^{-N}}. \quad (16)$$

The resulting discrete difference (14) characterizes a relation between the output and excitation of the system under investigation, thus allowing us to replace it with a model formed with (14) and then to simulate it.

B. Identification of ARMA Coefficients

In order to identify coefficients a_i and b_i of the transfer function $H(z)$, or, equivalently, the coefficients of the linear difference equation (14), we write (14) for each time-domain sample

t_k ($k = 1 \dots K$) which gives [11] the following overdetermined linear system:

$$[Y \ -U] \begin{bmatrix} \underline{a} \\ \underline{b} \end{bmatrix} = \begin{bmatrix} -y(t_1) \\ -y(t_2) \\ \vdots \\ -y(t_K) \end{bmatrix}. \quad (17)$$

Vectors \underline{a} and \underline{b} collect the set of coefficients to be determined while Y and U are known matrices that assemble the output response and excitation evaluated at each time step according to (14). Equation (17) is solved in the least-squares (LS) sense.

C. Conversion of ARMA Model to s -Domain

The ARMA model can be made applicable for an arbitrary time step by converting it into the continuous s -domain. For that purpose, we use the Matlab function `residue.m` for transforming the polynomial form (16) into the pole-residue form (12). Finally, the coefficients of the rational model (12) in the z -domain are transformed into the s -domain (3a) by the expressions in Table I. Note, however, that in the case of high-order approximations, the conversion from the polynomial form (16) to the pole-residue form (12) can lead to errors in the model's response [20].

V. Z-DOMAIN VECTOR FITTING (ZD-VF)

A. Formulation of Vector Fitting in z -Domain

The frequency-domain VF algorithm [9] (FD-VF) can be directly applied also to the z -domain transfer functions, giving poles and residues of a z -domain rational function $H(z)$ (12) that best fits the original data $\hat{H}(z_i)$ [13]. The given transfer function ($z_i, \hat{H}(z_i)$), the starting point, is conveniently specified on the boundary of the z -domain unitary circle.

As with FD-VF, the response data $\hat{H}(z)$ is multiplied (18) with an unknown rational scaling function $\sigma(z)$, where the poles of $\sigma(z)$ and the right side are assigned a set of initial values $q_{n,z}$. Equation (18) is solved as a linear LS problem. It can then be shown [9] that the zeros of $\sigma(z)$ must be a good approximation for the poles of $H(z)$. By repeating the procedure with the new poles replacing the initial poles, the poles will approach the correct pole set $p_{n,z}$ (12). Any unstable pole (outside the z -domain unitary circle) is enforced to be stable by flipping inside the unit circle [13]. The initial poles $q_{n,z}$ are chosen inside the stable z -domain unit circle and possibly close to its boundary. In practice, one may specify the poles in the s -domain as in [9] (complex conjugate, small real parts, and distributed along the imaginary axis), and then transform the poles into the z -domain by (6)

$$\overbrace{\left(1 + \sum_{n=1}^N \frac{c_n}{z - q_{n,z}}\right)}^{\sigma(z)} \hat{H}(z) = m_\infty + \sum_{n=1}^N \frac{m_n}{z - q_{n,z}}. \quad (18)$$

Finally, with the final pole set $p_{n,z}$, the residues $r_{n,z}$ are computed by solving (18) with $\sigma(z)$ set to unity.

B. Z-Transfer Function from Time-Domain Responses

In our case, the inputs are the time-domain responses obtained by a circuit simulator. We apply an approximation (19) to the Dirac's delta function, thereby obtaining an approximation $h^*(t)$ of the impulse transfer function

$$\delta^*(t) = \begin{cases} 0 & t \neq 0 \\ 1/\Delta t & t = 0 \end{cases} \quad (19)$$

Using the CZT algorithm (Section III-C), the impulse response in the z -domain $\hat{H}(z_i)$ is directly obtained. The points $z_i, i = 0 \dots M-1$, on which we evaluate the z -transform of $h^*(t)$, are chosen on a part of the unitary circle defined by an angle between $(-\theta_M, +\theta_M)$ where

$$\theta_M = 2\pi f_{\max} \Delta t \quad (20)$$

and f_{\max} is the highest frequency of interest in the (discrete) time-domain data. When applied with the CZT transformation (11), we use in (9) $\beta_0 = -\theta_M/(2\pi)$ and $\varphi_0 = -2\theta_M/[2\pi(M-1)]$.

At this point, we can finally apply the ZD-VF in order to estimate poles and residues of the transfer function $H(z)$ (12).

C. Recovering s -Domain Rational Function

Once the transfer function $H(z)$ has been expressed as a rational fraction expansion in the z -domain (12), the equivalent poles and residues in the s -domain are recovered by the expressions in Table I.

VI. TIME-DOMAIN VECTOR FITTING (TD-VF)

A. Formulation in the Frequency Domain

The FD-VF [9] can also be applied to time-domain responses via convolution, as shown in [14]. This is achieved by first introducing the input $U(s)$ and output $Y(s)$ in the pole identification step for VF as shown in (21), where $\{q_{n-s}\}$ is a set of initial poles

$$\overbrace{\left(1 + \sum_{n=1}^N \frac{k_n}{s - q_{n-s}}\right)}^{\sigma(s)} Y(s) = \left(\sum_{n=1}^N \frac{m_n}{s - q_{n-s}} + m_\infty\right) U(s). \quad (21)$$

Reordering (21) and simplifying the notation gives

$$Y(s) = \sum_{n=1}^N m_n \tilde{U}_n(s) - \sum_{n=1}^N k_n \tilde{Y}_n(s) + m_\infty U(s) \quad (22)$$

with

$$\tilde{U}_n(s) = \frac{1}{s - q_{n-s}} U(s) \quad (23)$$

$$\tilde{Y}_n(s) = \frac{1}{s - q_{n-s}} Y(s). \quad (24)$$

B. Formulation in Time Domain (TD-VF)

In our application, $u(t)$ and $y(t)$ are given in the time domain. Applying the inverse Laplace operator to both sides of (22) gives [14]

$$y(t) = \sum_{n=1}^N m_n \tilde{u}_n(t) - \sum_{n=1}^N k_n \tilde{y}_n(t) + m_\infty u(t) \quad (25)$$

where the definition of $\tilde{u}_n(t)$ and $\tilde{y}_n(t)$ depends on the applied numerical integration method. In order to solve for the unknowns $\{m_n\}$, $\{k_n\}$ and m_∞ , we write (25) for each sample $t_k = k\Delta t$, where Δt is the time step. This gives an overdetermined linear system that is solved in the LS sense. From the obtained $\{k_n\}$, the new poles $\{q_{n-s}\}$ are estimated as the zeros of $\sigma(s)$ [9]. This pole-relocation procedure is repeated iteratively where the calculated poles are used as new initial poles.

Once the final poles $\{q_{n-s}\}$ have been extracted, the residues are calculated by writing (26) as an overdetermined system and solving for the unknowns r_{n-s}

$$y(t) = \sum_{n=1}^N r_{n-s} \tilde{u}_n(t) + r_{0-s} u(t). \quad (26)$$

C. Numerical Integration

Alternative ways can be used for obtaining $\tilde{u}_n(t)$ and $\tilde{y}_n(t)$ from (23) and (24). We show the result only for the derivation of $\tilde{u}_n(t)$ because the procedure for $\tilde{y}_n(t)$ follows the same steps.

Equation (23) can be rewritten as (27) which can be brought into the time domain by the differential equation (28)

$$s\tilde{U}_n(s) = q_{n-s}\tilde{U}_n(s) + U(s) \quad (27)$$

$$\frac{d}{dt}\tilde{u}_n(t) = q_{n-s}\tilde{u}_n(t) + u(t). \quad (28)$$

Introducing discretization permits solving (28) using a numerical integration method. In the original formulation of TD-VF [14], the ‘‘recursive convolution’’ [21] was adopted. However, available circuit simulators are usually based on other integration methods (e.g., trapezoidal integration) and so a mismatch exists between the integration scheme of the circuit solver and TD-VF. In what follows, we show how to incorporate the trapezoidal integration method into TD-VF.

The trapezoidal method implies the following discretization (29) of (28):

$$\frac{\tilde{u}_n(t_k) - \tilde{u}_n(t_{k-1})}{\Delta t} = q_{n-s} \frac{\tilde{u}_n(t_k) + \tilde{u}_n(t_{k-1})}{2} + \frac{u(t_k) + u(t_{k-1})}{2}. \quad (29)$$

Thus, it is straightforward to write the discrete solution of (28) on the form (30) with coefficients given by (31)

$$\tilde{u}_n(t_k) = \alpha_n \tilde{u}_n(t_{k-1}) + \lambda_n u(t_k) + \mu_n u(t_{k-1}) \quad (30)$$

$$\alpha_n = \frac{1 + q_{n-s} \frac{\Delta t}{2}}{1 - q_{n-s} \frac{\Delta t}{2}}, \quad \lambda_n = \mu_n = \frac{\frac{\Delta t}{2}}{1 - q_{n-s} \frac{\Delta t}{2}}. \quad (31)$$

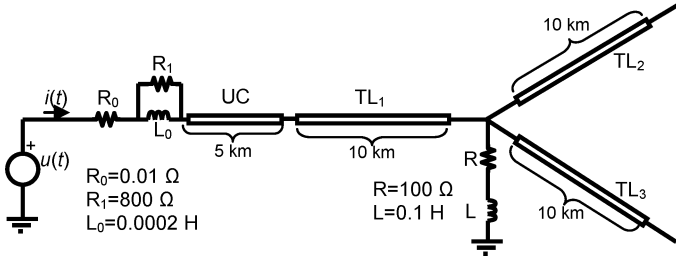


Fig. 1. Single-phase power system.

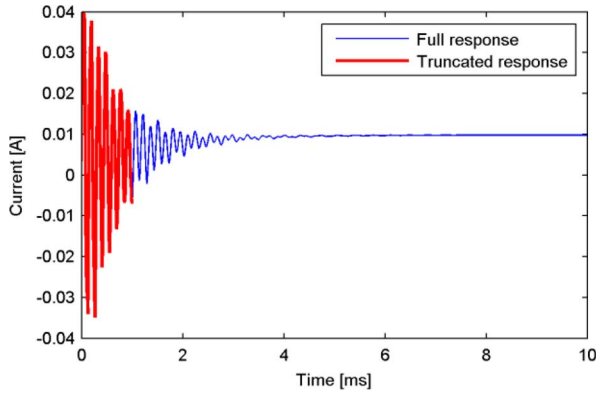


Fig. 2. Simulated current response (PSCAD).

VII. EXAMPLE: FREQUENCY-DEPENDENT NETWORK EQUIVALENT (FDNE)

A. Problem Statement

We consider the single-phase power system in Fig. 1 which is composed of an underground cable and three identical overhead lines. We refer to [22] for the geometry of the single-core underground cable and the overhead line.

In what follows, we apply all methods for identifying a rational model (3a) of the admittance transfer function $Y(s)$ of the system as seen from the voltage source in Fig. 1. The following notation is adopted:

- 1) ARMA_dde: discrete difference equation model obtained by solving (17), and applicable for the same time-step of the original data;
- 2) ARMA_pfe: model obtained by converting the discrete difference equation into the s -domain [partial fraction expansion form (3a)];
- 3) ZD-VF: model obtained by applying the z -domain vector fitting algorithm.
- 4) TD-VF: model obtained by applying the time-domain vector fitting algorithm.

With all approaches, the linear LS problems [(17), (18), (25), (26)] are solved by using the backslash operator (“\”) in Matlab.

The current response due to a unit step voltage application is shown in Fig. 2. For the purpose of model extraction, we will use two alternative window lengths: 1 ms and 10 ms.

B. Computation of Time-Domain Responses

Using the trapezoidal-based circuit solver PSCAD, we apply two different voltage excitations $u(t)$ to the network shown in

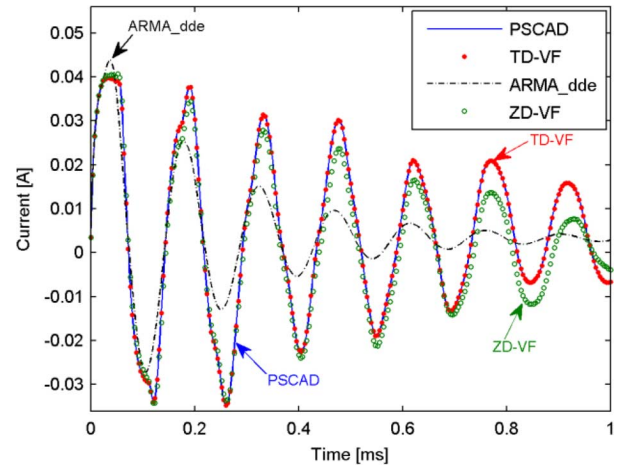
Fig. 3. Current response. Original PSCAD simulation and simulation by models extracted by using TD-VF, ARMA_dde, and ZD-VF. $N = 20$.

Fig. 1 with a fixed time step of $1 \mu\text{s}$ and record the current response $i(t)$ flowing into the network. The first excitation is a unit step while the second is an approximation of the Dirac’s delta function (19). The first excitation/response is used as input data for TD-VF and ARMA_dde/pfe while the second excitation/response is used with ZD-VF.

C. Base Case Results

The TD-VF and ZD-VF approaches are applied with 30 pole relocating iterations, using a time step length of $1 \mu\text{s}$ and a window length 1 ms (1000 samples). All approaches (including ARMA) are applied with a fitting order $N = 20$. With ZD-VF, the mapping from the time domain to z -domain is accomplished using 5000 samples to achieve a high resolution, and we use an angle of $\pm 150^\circ$. The quality of the extracted models is then compared by applying the model in a numerical simulation with step voltage excitation. That simulation is done using an EMTP-like simulation in Matlab based on trapezoidal integration [23], again with a $1\text{-}\mu\text{s}$ time step.

The results are shown in Fig. 3, comparing the original PSCAD simulation of the input current $i(t)$ with the one obtained using the respective models. It is seen that only the model extracted by TD-VF gives a good match with the original data. Both the ARMA_dde and ZD-VF models give poor results. (The result by ARMA_pfe is similar to that of ARMA_dde.)

Fig. 4 shows the simulated voltage responses when the voltage source is replaced by a unit step current source. Again, the result by TD-VF gives an accurate result while the other approaches lead to a highly inaccurate result.

As a final comparison, the admittance transfer functions are plotted in the frequency domain, see Fig. 5 and an expanded view in Fig. 6. The responses are compared with the admittance obtained by PSCAD directly in the frequency domain. It can be seen that TD-VF attains the best result in the frequency band (1 kHz–1 MHz) that is associated with the time window used for model extraction ($1 \mu\text{s}$ –1 ms). Outside this window, the accuracy deteriorates due to a lack of information in the time-domain responses. The other approaches (ARMA, ZD-VF) give

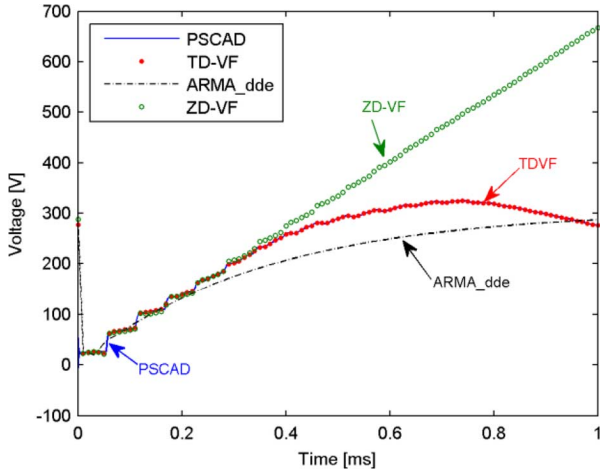


Fig. 4. Voltage response. Original PSCAD simulation and simulation by models extracted by using TD-VF, ARMA_dde, and ZD-VF. $N = 20$.

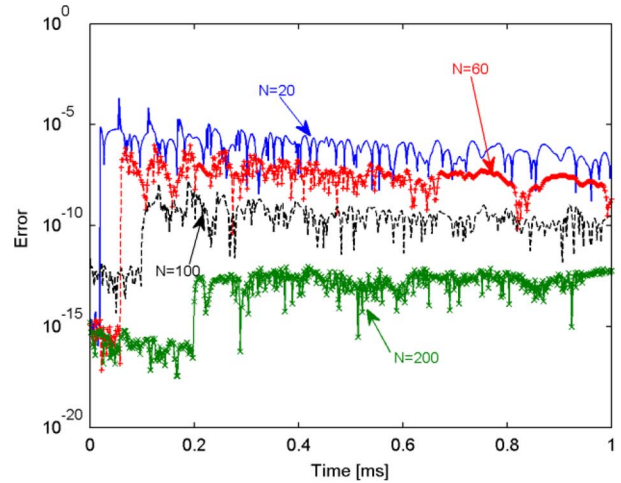


Fig. 7. Error curves for the identification of ARMA coefficients (17) with alternative model orders $N = 20, 60, 100, 200$.

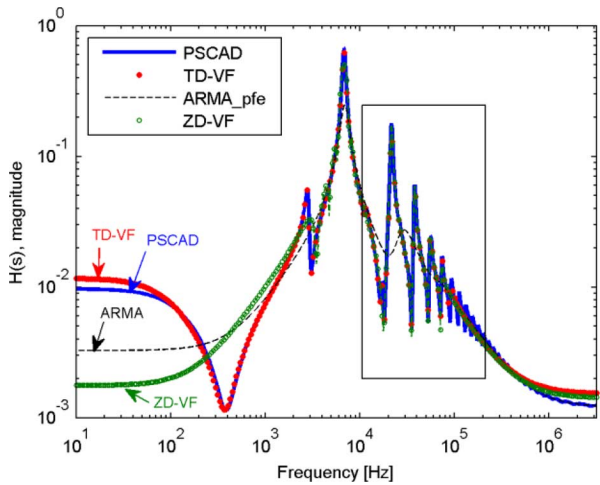


Fig. 5. Frequency-domain impulse response. Original PSCAD model and models extracted by TD-VF, ARMA_pfe and ZD-VF.

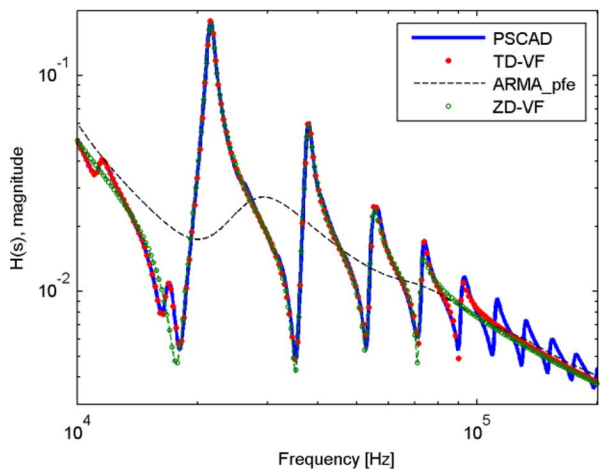


Fig. 6. Expanded view of Fig. 5 (inset box).

substantial deviations also within the (1 kHz–1 MHz) frequency band, consistent with the result in Fig. 3.

D. ARMA: Further Results

In this section, we further elaborate on the difficulties with the ARMA modeling procedure.

Fig. 7 shows the error in the solution of the linear problem (17), for different fitting orders. Since the right side in (17) is directly equal to the output response (which, in our case, is the current response due to a step voltage excitation), the traces in Fig. 7 directly correspond to the model error with the given excitation. All models give an error smaller than $1E-5$, and the error is close to machine precision for the first N time samples where N is the model order. The error is reduced with increasing fitting order.

Fig. 8 shows the error of the ARMA models in Fig. 7 when applied in the simulation (current response due to a step voltage excitation). The deviations are now much higher than in Fig. 7. Only the 200-order approximation gives a highly accurate result. The reason for the increased error can be understood as follows. When building the linear problem (17), the output (current response) is used for the building of the system matrix. When applying the model in a simulation, the output response is slightly perturbed by the model inaccuracies. That way, the model perturbs itself, leading to a deviation that increases with time.

Even when using very high orders, the performance of the ARMA model is often unacceptable. Fig. 9 shows an example where the ARMA model is applied with an order of 180. It is observed that the simulation using ARMA gives very good agreement until $t = 0.6$ ms, but then becomes unstable. The reason for the unstable result can be explained by unstable poles. Unlike the TD-VF and ZD-VF approaches, the ARMA method cannot enforce stable poles by construction.

In order to make the ARMA model applicable with arbitrary time steps, it can be converted into a rational model using the procedure described in Section IV-C. The simulation result using the “rational” ARMA model is shown in Fig. 10 with alternative fitting orders, also with a $1-\mu\text{s}$ time step. It is seen that all models produce unacceptable results. The reason for the problems is that the conversion from the discrete ARMA model to

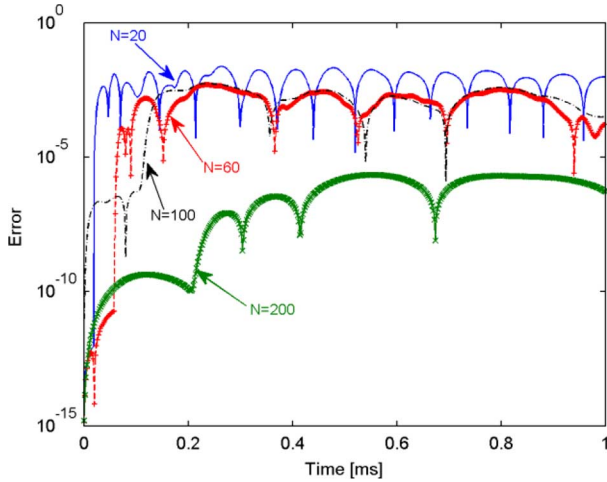


Fig. 8. Error curves for simulated current response using ARMA_dde models of alternative orders $N = 20, 60, 100, 200$.

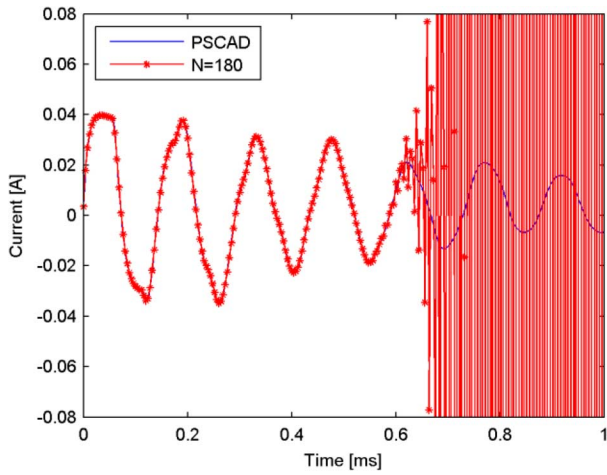


Fig. 9. Comparison between the original current obtained with PSCAD and simulated unstable ARMA_dde model with order 180.

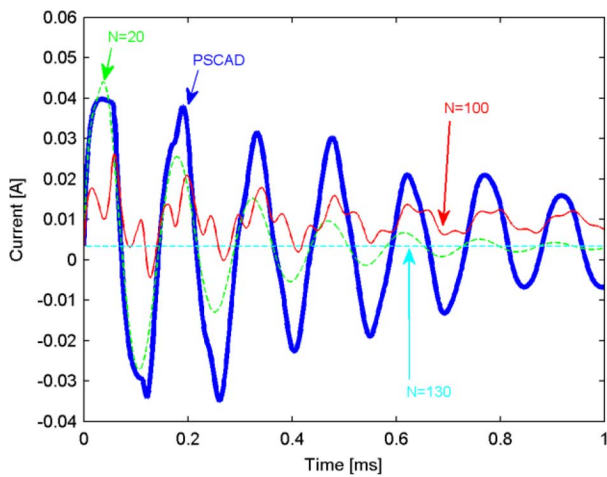


Fig. 10. Comparison between the original current obtained with PSCAD and simulated ARMA_pfe models with alternative fitting orders: $N = 20, 100, 130$.

the rational ARMA model on the partial fraction expansion form (12) is unreliable due to numerical ill-conditioning [20].

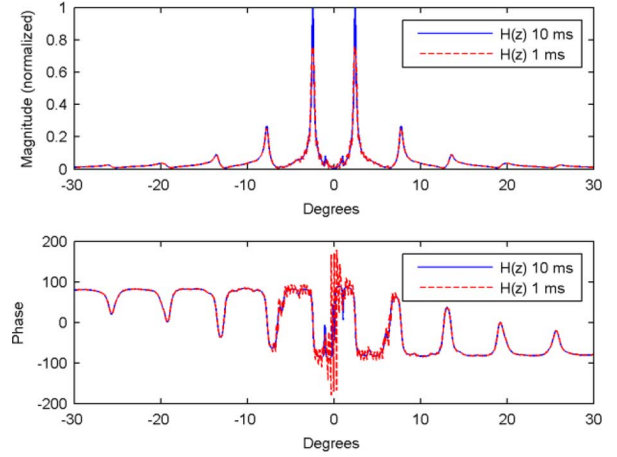


Fig. 11. Comparison between a z -transfer function of a non-truncated (10 ms) signal and truncated signal (1 ms).

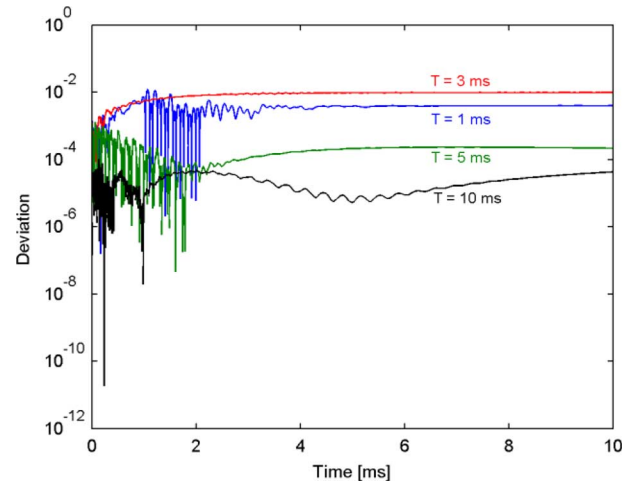


Fig. 12. Fitting error between the simulated z -domain vector fitting applied to PSCAD data obtained for four different window time lengths. $N = 40$.

E. ZD-VF: Further Results

The errors in the simulation by ZD-VF (Fig. 3) are mainly due to the truncated nature of the time signal $i(t)$ used as the input for the modeling process. The truncation of $i(t)$ leads to inaccurate computation of the z -domain response. The error is greatly reduced by increasing the length of the time window until the response $i(t)$ has decayed to zero.

Fig. 11 shows the magnitude and phase angle of the z -domain response used as input for ZD-VF, when the simulation end is at either 1 ms (used in this study) or 10 ms. It can be seen that with the 1-ms window, oscillations result in the calculated response that are not observable with the 10-ms window.

Fig. 12 shows the deviation of the ZD-VF model with alternative lengths of the time window. It is seen that the error decreases with an increasing time window.

F. TD-VF: Further Results

The TD-VF was in Section VII-C found to produce an excellent result with a low-order approximation ($N = 20$), both for a step voltage excitation and a step current excitation. Fig. 13

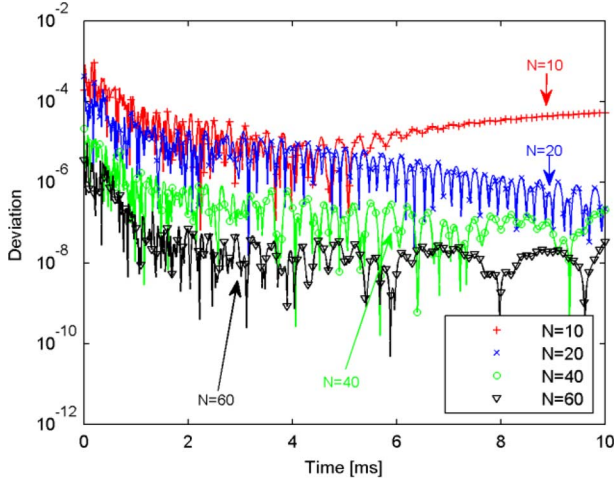


Fig. 13. Error curves for simulated current response using TD-VF models of alternative orders $N = 10, 20, 40, 60$.

shows the deviation of the simulation result by TD-VF for alternative fitting orders, based on a 10-ms time window for the fitting process. It is observed that the error is consistently reduced with increasing fitting orders. The deviation with $N = 40$ is directly comparable with the result for ZD-VF in Fig. 12. It can be seen that TD-VF gives a substantially lower error. This result can be related to the usage of the bilinear transformation for mapping the model from the z -domain to the s -domain. In addition, a small truncation effect will be present since the response is not entirely zero at 10 ms (0.0098 A).

We next demonstrate the applicability of the TD-VF model for use with alternative time step lengths. A 20th-order model is extracted by TD-VF based on a PSCAD simulation of the voltage excitation response, assuming a $1\text{-}\mu\text{s}$ time step and 1-ms time window.

Fig. 14 compares the simulation result by the TD-VF model and PSCAD when employing a $\Delta t = 5\ \mu\text{s}$ time step in both simulations. A noticeable deviation appears between all three traces. The reason for the deviations can be explained as follows.

- 1) The change in the PSCAD simulation result is mainly due to increased interpolation errors in the traveling-wave model. This type of error results when the time delay τ is not an integer multiple of Δt while at the same τ is not much bigger than Δt . In this case, τ is $28.1\ \mu\text{s}$ for the cable and $33.5\ \mu\text{s}$ for each of the overhead lines.
- 2) The reason for the error in the simulation result by TD-VF is mainly a result of the integration method. In the simulation by TD-VF, trapezoidal integration was employed while the traveling-wave model in PSCAD is based on recursive convolution [21]. Therefore, the nature of the integration errors is different.

Fig. 15 shows the same result as in Fig. 14 when Δt has been increased to $5.62\ \mu\text{s}$ and the trapezoidal integration method has been replaced with recursive convolution in the simulation of the TD-VF model. With these modifications, all approaches give virtually the same result. Note that with $\Delta t = 5.62\ \mu\text{s}$, τ of the cable and line is, respectively, 5.0 and 6.0 times bigger than Δt .

In general, however, the model extracted by TD-VF cannot avoid that the integration method causes errors in the simula-

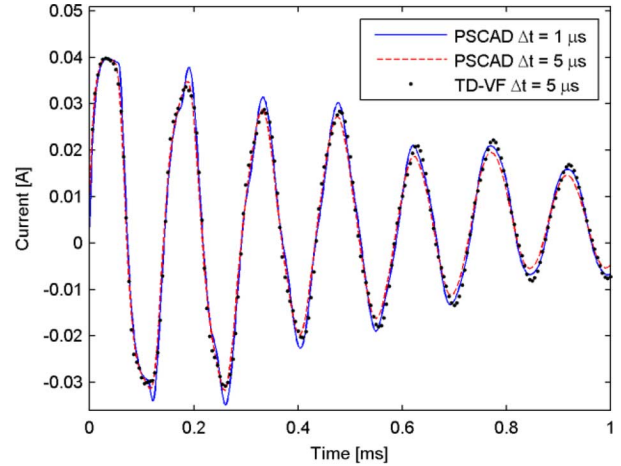


Fig. 14. Comparison between PSCAD responses ($1\ \mu\text{s}$ and $5\ \mu\text{s}$) and simulated TD-VF model ($5\ \mu\text{s}$). $N = 20$.

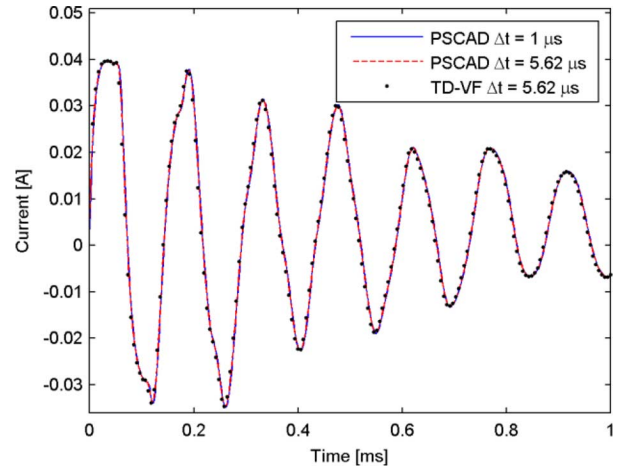


Fig. 15. Comparison between PSCAD responses ($1\ \mu\text{s}$ and $5.62\ \mu\text{s}$) and simulated TD-VF model ($5.62\ \mu\text{s}$). $N = 20$. TD-VF model simulated by recursive convolution.

tion result. Therefore, the accuracy will often deteriorate when increasing the time step.

We have also observed that the simple pole flipping scheme [9] is not always successful for TD-VF since the VF iteration may not converge. A simple remedy is to extend the length of the time window to capture a full period of the lowest frequency component observable in the data.

G. Results With Modified Circuit

We now modify the network in Fig. 1 by reducing the inductance from 200 to $2\ \mu\text{H}$. As a result, the current response becomes much less smooth. When applying the same time step ($1\ \mu\text{s}$) and window length (1 ms) as before for the model extraction process, the ARMA and ZD-VF models all fail to produce an acceptable simulation result. The TD-VF approach still produces a sufficiently accurate result, although a higher order is now required in order to capture the increased frequency content.

Fig. 16 shows the result obtained with TD-VF using 80 poles. The extracted model gives a simulation result matching the original PSCAD data quite accurately at the given time samples. The same plot also shows the analytical response of the model with

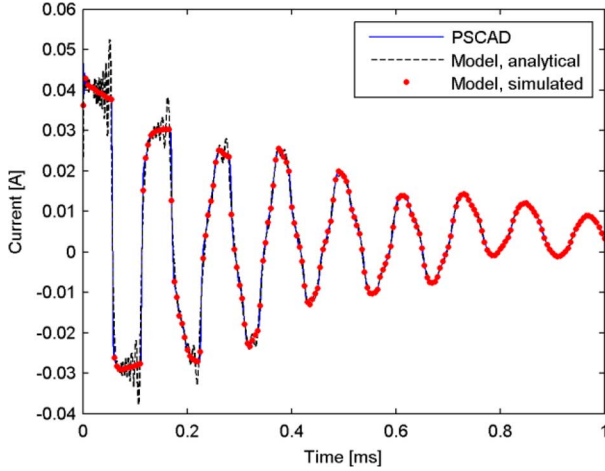


Fig. 16. Comparison between the original current response by PSCAD and response by TD-VF model: analytical and simulation. $N = 80$.

TABLE III

COMPUTATION TIME FOR A SINGLE TD-VF ITERATION (in milliseconds)

Model order	$N=20$	$N=40$	$N=60$	$N=80$
Building system matrix	1.5	2.6	3.7	4.9
Solving linear problem	2.4	7.7	15.9	23.8

a very fine time resolution. That response is highly oscillatory and will eventually be captured by the model when reducing the time step in the simulation (i.e., below $1 \mu\text{s}$). The oscillations occur because the fitting process, gives a bandlimited model that fails to capture the frequency components beyond 1 Mz , thereby giving Gibbs-like oscillations in the response.

H. Complexity Analysis

We consider now some aspects regarding timing requirements for the described methods.

With each of these approaches—ARMA, TD-VF and ZD-VF—a linear system has to be solved in the least-squares sense. The system matrix size is the same for all methods, being $K \times (2N + 1)$, where N is the order and K is the number of time-domain (or z -domain) samples. It is found that most of the CPU time is spent in the solution of the linear system equation. This operation is completed a single time for ARMA and repeatedly for TD-VF and ZD-VF. In addition, in each iteration of TD-VF, another $10NK$ operations are needed for establishing the coefficients of the system matrix. That time, however, is negligible with high-order approximations, see Table III. It can thus be concluded that ARMA is faster than the other approaches since pole relocations are not needed. In the examples, we used 30 iterations with ZD-VF and TD-VF, but, in practice, one will normally use much fewer iterations, often as few as 3–5 iterations.

VIII. MULTIPHASE EXAMPLE

TD-VF is also applicable to multiport systems. For illustration, we apply the approach to a subnetwork of five three-phase

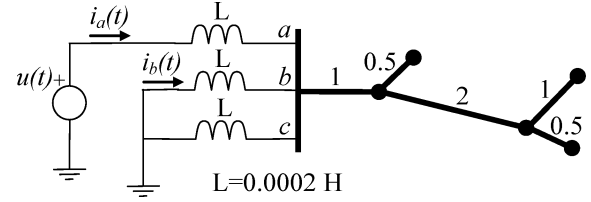


Fig. 17. Three-phase power system. The length of the lines is given in kilometers.

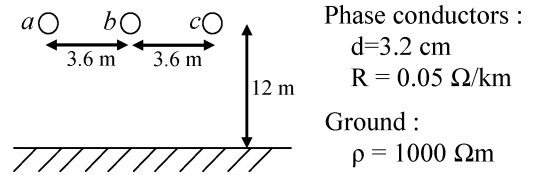


Fig. 18. Geometry of the overhead lines for the power system of Fig. 17.

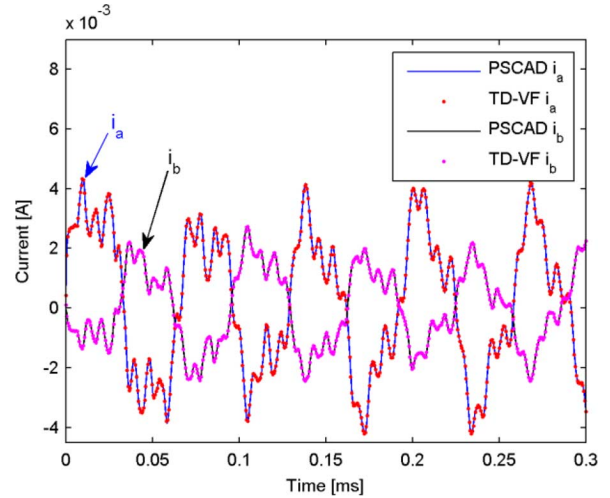


Fig. 19. Comparison between original current responses (i_a and i_b) by PSCAD ($0.1 \mu\text{s}$) and simulated TD-VF model ($0.1 \mu\text{s}$). $N = 40$.

overhead lines having different line lengths but the same geometry, see Figs. 17 and 18.

Similar to the previous example, we apply the circuit solver PSCAD in order to compute the time-domain responses (phase currents flowing into the network) using a step voltage as excitation. The voltage is applied to phase a with phases b and c grounded. We use a time step of $0.1 \mu\text{s}$ and a window length of 0.3 ms . The TD-VF approach is then applied using 30 iterations with a fitting order $N = 40$. Fig. 19 compares the original response with the one simulated using the extracted model. The result is shown for the current in phase a and b . It can be seen that a highly accurate result is achieved.

We remark that in this modeling/simulation, we have represented the subnetwork by one diagonal element (Y_{aa}) and one offdiagonal element (Y_{ba}). We are currently extending the modeling capability to handle vectors of responses so as to arrive at a complete, coupled model with a common poles set for all matrix elements.

IX. CONCLUSION

In this work we have compared alternative methods for obtaining a rational approximation from simulated time-domain responses. These approaches are based on ARMA, ZD-VF, and TD-VF.

ARMA, which is based on the discrete difference equation, gives a model which is applicable only with the same time step as the one in the given time-domain data. The approach leads to higher model orders than the alternative approaches, and it cannot guarantee stable poles. In this work we introduced a procedure for converting the ARMA model into a general rational model, making it applicable to general time steps. That approach was found to suffer from inaccurate results due to numerical robustness problems in the conversion process from polynomial form to pole-residue form.

ZD-VF is not directly applicable to time-domain responses. It requires an initial transformation of the time-domain responses into the z -domain. The resulting z -domain response becomes corrupted when applied to time-domain responses that are not sufficiently decayed to zero within the time window. This corruption results in an inaccurate model. Also, the final conversion of the z -domain rational model back to the continuous time domain will introduce some error due to the application of the bilinear transformation. ZD-VF has the advantage over ARMA that it is robust and gives a model with guaranteed stable poles.

TD-VF is the best option for rational modeling from time-domain responses. It allows to use truncated responses, it requires a much lower model order than ARMA, it gives a model with guaranteed stable poles, and it is robust. The obtained model can be used with an alternative time step length as long as it stays within the limits implied by the step length and window length of the given time data series, and the limitations implied by the numerical integration method.

REFERENCES

- [1] H. W. Dommel and W. S. Meyer, "Computation of electromagnetic transients," *Proc. IEEE*, vol. PROC-62, no. 7, pp. 983–993, Jul. 1974.
- [2] J. R. Marti, "Accurate modelling of frequency-dependent transmission lines in electromagnetic transient simulations," *IEEE Trans. Power App. Syst.*, vol. PAS-101, no. 1, pp. 147–157, Jan. 1982.
- [3] A. Morched, B. Gustavsen, and M. Tartibi, "A universal model for accurate calculation of electromagnetic transients on overhead lines and underground cables," *IEEE Trans. Power Del.*, vol. 14, no. 3, pp. 1032–1038, Jul. 1999.
- [4] T. Noda, N. Nagaoka, and A. Ametani, "Phase domain modeling of frequency-dependent transmission lines by means of ARMA model," *IEEE Trans. Power Del.*, vol. 11, no. 1, pp. 401–411, Jan. 1996.
- [5] A. Morched, L. Marti, and J. Ottevangers, "A high frequency transformer model for the EMTP," *IEEE Trans. Power Del.*, vol. 8, no. 3, pp. 1615–1626, Jul. 1993.
- [6] B. Gustavsen, "Wide band modeling of power transformers," *IEEE Trans. Power Del.*, vol. 19, no. 1, pp. 414–422, Jan. 2004.
- [7] A. Morched, J. Ottevangers, and L. Marti, "Multi-port frequency dependent network equivalents for the EMTP," *IEEE Trans. Power Del.*, vol. 8, no. 3, pp. 1402–1412, Jul. 1993.
- [8] M. Abdel-Rahman, A. Semlyen, and R. Iravani, "Two-layer network equivalent for electromagnetic transients," *IEEE Trans. Power Del.*, vol. 18, no. 4, pp. 1328–1335, Oct. 2003.
- [9] B. Gustavsen and A. Semlyen, "Rational approximation of frequency domain responses by vector fitting," *IEEE Trans. Power Del.*, vol. 14, no. 3, pp. 1052–1061, Jul. 1999.
- [10] H. Singh and A. Abur, "Multi-port equivalencing of external systems for simulation of switching transients," *IEEE Trans. Power Syst.*, vol. 10, no. 1, pp. 374–382, Jan. 1995.
- [11] W. D. C. Boaventura, A. Semlyen, M. R. Iravani, and A. Lopes, "Sparse network equivalent based on time-domain fitting," *IEEE Trans. Power Del.*, vol. 17, no. 1, pp. 182–189, Jan. 2002.
- [12] T. Henriksen, "Including high order rational functions in EMTP, a comparison between alternative methods with emphasis on accuracy," *IEEE Trans. Power Del.*, vol. 12, no. 1, pp. 372–378, Jan. 1997.
- [13] Y. S. Mekonnen and J. E. Schutt-Ainé, "Fast macromodeling technique of sampled time/frequency data using z -domain vector-fitting method," in *Proc. IEEE Electrical Performance of Electronic Packaging*, 2007, pp. 47–50.
- [14] S. Grivet-Talocia, "Package macromodeling via time-domain vector fitting," *IEEE Trans. Microw. Wireless Compon. Lett.*, vol. 13, no. 11, pp. 472–474, Nov. 2003.
- [15] C. L. Phillips, J. M. Parr, and E. A. Riskin, *Signals, Systems, and Transforms*, 4th ed. Upper Saddle River, NJ: Prentice-Hall, 2008.
- [16] D. Brook and R. J. Wynne, *Signal Processing, Principles and Applications*. London, U.K.: Edward Arnold, 1988.
- [17] T. Noda and A. Ramirez (IEEE Power Engineering Society Task Force on Frequency Domain Methods for Transient Studies, Working Group on Modeling and Analysis of System Transients Using Digital Simulation, General Systems Subcommittee), "Z-transform-based methods for electromagnetic transient simulations," *IEEE Trans. Power Del.*, vol. 22, no. 3, pp. 1799–1805, Jul. 2007.
- [18] J. G. Proakis and D. G. Manolakis, *Digital Signal Processing*, 4th ed. Upper Saddle River, NJ: Prentice-Hall, 2008.
- [19] N. Watson and J. Arrillaga, *Power Systems Electromagnetic Transients Simulation*, ser. IET Power and Energy Series 39. London, U.K.: Inst. Eng. Technol., 2007.
- [20] Mathworks, Inc., Matlab documentation. R2009a. [Online]. Available: <http://www.mathworks.com>
- [21] A. Semlyen and A. Dabuleanu, "Fast and accurate switching transient calculations on transmission lines with ground return using recursive convolutions," *IEEE Trans. Power App. Syst.*, vol. PAS-94, no. 2, pp. 561–575, Mar./Apr. 1975.
- [22] A. Ramirez, "Vector fitting-based calculation of frequency-dependent network equivalents by frequency partitioning and model-order reduction," *IEEE Trans. Power Del.*, vol. 24, no. 1, pp. 410–415, Jan. 2009.
- [23] B. Gustavsen and O. Mo, "Interfacing convolution based linear models to an electromagnetic transients program," in *Proc. Int. Conf. Power Systems Transients*, Lyon, France, Jun. 4–7, 2007, p. 6.

Andrea Ubolli (M'10) received the Laurea and Ph.D. degrees in electronic engineering from the Politecnico di Torino, Torino, Italy, in 2003 and 2008, respectively.

In 2004, since graduation, he joined the Electromagnetic Compatibility Group in the Department of Electronics of the Politecnico di Torino, Torino, Italy, as a Research Assistant, working on interconnect macromodeling and aiding in the development of the IdEM tool. From 2005 to 2008, he was a Ph.D. student working on the robust passive macromodeling of signal and power distribution networks in high-speed electronic systems. In 2009, he was the recipient of a Lagrange Project Scholarship, supporting his research on complex systems modeling. Since 2009, he has been a Postdoctoral Researcher with SINTEF Energy Research in cooperation with the University of Trondheim, Trondheim, Norway, where he is working on frequency-dependent modeling of power systems.

Bjørn Gustavsen (M'94–SM'03) was born in Norway in 1965. He received the M.Sc. degree and Dr.ing. degrees from the Norwegian Institute of Technology (NTH), Trondheim, in 1989 and 1993, respectively.

Since 1994, he has been with SINTEF Energy Research, where he is currently a Senior Research Scientist. His interests include the simulation of electromagnetic transients and modeling of frequency-dependent effects. He spent 1996 as a Visiting Researcher at the University of Toronto, Toronto, ON, Canada, and the summer of 1998 at the Manitoba HVDC Research Centre, Winnipeg, MB, Canada.

Dr. Gustavsen was a Marie Curie Fellow at the University of Stuttgart, Stuttgart, Germany, from 2001 to 2002.